J Mol Model (2008) 14:761–768
DOI 10.1007/s00894-008-0312-1

ORIGINAL PAPER

Regulatory phosphorylation of cyclin-dependent kinase 2: insights from molecular dynamics simulations

Iveta Bártová · Jaroslav Koča · Michal Otyepka

Received: 21 November 2007 / Accepted: 4 April 2008 / Published online: 10 May 2008

Abstract The structures of fully active cyclin-dependent kinase-2 (CDK2) complexed with ATP and peptide substrate, CDK2 after the catalytic reaction, and CDK2 inhibited by phosphorylation at Thr14/Tyr15 were studied using molecular dynamics (MD) simulations. The structural details of the CDK2 catalytic site and CDK2 substrate binding box were described. Comparison of MD simulations of inhibited complexes of CDK2 was used to help understand the role of inhibitory phosphorylation at Thr14/Tyr15. Phosphorylation at Thr14/Tyr15 causes ATP misalignment for the phosphate-group transfer, changes in the Mg^{2+} coordination sphere, and changes in the H-bond network formed by CDK2 catalytic residues (Asp127, Lys129, Asn132). The inhibitory phosphorylation causes the G-loop to shift from the ATP binding site, which leads to opening of the CDK2 substrate binding box, thus probably weakening substrate binding. All these effects explain the decrease in kinase activity observed after inhibitory phosphorylation at Thr14/Tyr15 in the G-loop. Interaction of the peptide substrate, and the phosphorylated peptide product, with CDK2 was also studied and compared. These results broaden hypotheses drawn from our previous MD studies as to why a basic residue (Arg/Lys) is preferred at the P_{+2} substrate position.

I. Bártová (✉) · M. Otyepka (✉)
Department of Physical Chemistry and Centre for Biomolecular and Complex Molecular Systems, Palacký University,
tr. Svobody 26,
771 46 Olomouc, Czech Republic
e-mail: iveta.bartova@upol.cz
e-mail: otyepka@aix.upol.cz

I. Bártová · J. Koča
National Centre for Biomolecular Research, Faculty of Science, Masaryk University,
Kamenice 5, A-4,
625 00 Brno, Czech Republic

Keywords CDK regulation · Protein substrate · Phosphorylation · Cell cycle · Molecular dynamics simulations

Introduction

The cyclin-dependent kinases (CDKs) (EC 2.7.1.37) are the catalytic subunits of a large family of heterodimeric serine/threonine protein kinases, which are important for regulation of many biologically critical processes in eukaryotic cells (for example, CDK1, CDK2, and CDK4 are involved in cell cycle regulation) [1, 2]. Early studies in *Schizosaccharomyces pombe* demonstrated that Cdc2 (CDK1) Tyr15 phosphorylation directly regulates entry into mitosis and, therefore, is an important element in the control of the unperturbed cell cycle [3, 4]. In human cells, the mechanism of inhibition of CDK1/cyclin complexes by phosphorylation is conserved and plays a major role in cell cycle control across the G2/M phase [5]. Similarly, CDK2 is phosphorylated on Thr14 and Tyr15 during S and G2 phases by human Wee1-like kinase (WeeHu), and is dephosphorylated by Cdc25 [6–8]. In general, protein phosphorylation in eukaryotes is probably the most important regulatory event because many enzymes are switched "on" or "off" by phosphorylation and dephosphorylation. Therefore, it is not surprising that the eukaryotic protein kinase family is one of the largest gene families in all eukaryotes, accounting for 2–4% of all genes [9]. Kinase activities are substantially altered in many cells, e.g. cancer cells, thus explaining why insights into the mechanism of cell cycle regulation are so important to the understanding of deregulation and the consequent origin of several diseases. Due to this observed deregulation in many serious human diseases, CDKs are promising biological targets for

the design of new inhibitors in human medicine. CDK inhibitors have been tested for the treatment of many human diseases such as cancer, neurodegenerative disorders (e.g. Alzheimer's disease, amyotrophic lateral sclerosis and stroke), diabetes, cardiovascular disorders (e.g. atherosclerosis and restenosis), viral infections (e.g. HCMV, HIV and HSV), etc. [10, 11].

The majority of kinases contain a 250–300 amino acid residue catalytic domain whose structure and, in particular, key catalytic residues are highly or absolutely conserved within the protein kinase family [12]. The residues that are conserved in all protein kinases are Lys33, Glu51, Asp127, Lys129, Asn132, and Asp145 (numbering according to human CDK2). This domain comprises a binding pocket for ATP (less frequently GTP—guanosine-5'-triphosphate). The catalytic function of CDKs is phosphorylation of a substrate protein via transfer of the γ-phosphoryl group of ATP (the ATP is bound as a complex with a Mg^{2+} ion) to a threonine or serine of the target protein substrate (Fig. 1).

The activity of these enzymes is controlled by reversible protein phosphorylation, as well as synthesis and degradation of activator and inhibitor subunits. CDK2 is inactive as a monomer (Fig. 1a), in which an activation segment—a region of the protein called the T-loop (residues 152–170)—blocks the active site. CDK2 activation is a two-step process. The first step is binding of cyclin A or cyclin E, which causes the T-loop to move out of the active site resulting in partial activation of CDK2. Cyclin also decreases the flexibility of the T-loop [13], which could explain observations that phosphorylation at Thr160 is cyclin-dependent in vitro [14]. The critical CDK/cyclin complexes for cell cycle function are CDK2/cyclin E, which drives the cell across the G1/S-phase border, and CDK2/cyclin A, which mediates DNA replication. The second step of the CDK2 activation process comprises phosphorylation of CDK2 by CDK-activating kinase [CAK; CDK7/cyclin H(/Mat1) complex] at a specific threonine residue in the T-loop (Thr160 in CDK2), which fully activates the enzyme by changing the shape of the T-loop, thus improving the ability of the enzyme to bind its protein substrate [1, 15] (Fig. 1b). Phosphorylation of Thr160 by CAK stabilises the substrate binding site [16–18]. Thr160 phosphorylation leads to reconfiguration of the activation segment and, following this conformational change, the binding pocket for the substrate proline (from the P_{+1} substrate position, where subscripts denote amino acid positions in the substrate numbered from the phosphorylation residue P_0 with numbers increasing toward the C-terminus) is created [19].

Analysis of peptide libraries for CDK2 substrate preference has determined the sequence $X_{-1}(S/T)_0P_{+1}X^*_{+2}(K/R)_{+3}$ to be an optimal substrate. Here, S or T (serine or threonine) are phosphorylation residues, P denotes proline

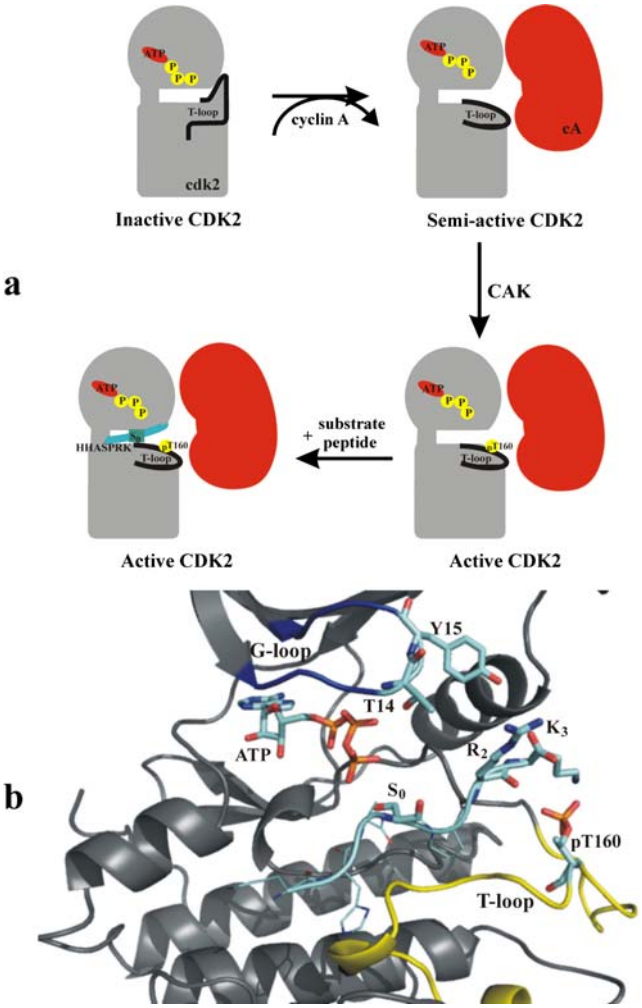

Fig. 1 **a** Illustration of the structure of human cyclin-dependent kinase-2 (CDK2) in complex with ATP in various activity states. Monomeric CDK2, in which the T-loop blocks the active site cleft, is inactive and its activation requires cyclin binding. For complete activation, CDK2 requires phosphorylation by CDK-activating kinase (CAK) at Thr160 in the T-loop. The substrate peptide (HHASPRK) binds between the T- and G-loops. **b** View of the substrate binding site of the fully active CDK2 (pT160-CDK2/cyclin A/ATP). The pThr160 activation site is located in the T-loop (*yellow secondary structure*). The G-loop, which partly forms the ATP binding site, is shown in *blue*. The Thr14 and Tyr15 inhibitory phosphorylation sites located in the G-loop are shown in *licorice representation*

at the P_{+1} substrate position, (K/R) is lysine or arginine at the P_{+3} substrate position, and *X* is any amino acid, but K/R (*X**) is favoured at the P_{+2} substrate position [20, 21]. Such comparative studies indicate that long aliphatic amino acids or a positively charged residue at the X^*_{+2} site contribute to the efficiency of peptide substrate phosphorylation. The functional/structural reason for these preferences remains unclear, because structural studies have not provided clear insights. The basic residue arginine at the X^*_{+2} position (denoted as residue R_{+2}) in the X-ray crystal structure of fully active CDK2 (pT160-CDK2/cyclin A/ATP) in complex with the substrate peptide (HHASPRK) (PDB ID:

1QMZ) makes no contacts with CDK2 and directs contact to the solvent. On the other hand, the lysine at the P_{+3} substrate position (denoted as K_{+3}) is H-bonded to the pThr160 phosphate and to the main-chain oxygen of residue Ile270 on cyclin A; these interactions explain the specificity for a basic residue at this position. The structure of fully active CDK2 in complex with the substrate peptide (HHASPRK) also explains other basic features of peptide binding to CDK2 [19]. The substrate peptide binds in an extended conformation across the catalytic site, and its binding site is located close to the active site on the C-terminal lobe surface. Some parts of the binding site are formed by the G-loop and T-loop of CDK2 (Fig. 1b). The T-loop forms a suitably shaped pocket to accept the substrate proline P_{+1} residue that lies next to the phosphorylation serine residue (S_0). CDKs display an absolute requirement for proline in the substrate P_{+1} position, hence the common reference to these enzymes as proline-directed kinases.

Materials and methods

Molecular dynamic (MD) simulations of fully active pT160-CDK2/cyclin A/ATP and pT160-CDK2/cyclin A/ATP/HHASPRK (active CDK2 in complex with peptide substrate HHASPRK), CDK2 inhibited by phosphorylation at the Thr14 or Tyr15 G-loop inhibitory sites (pT14pT160-CDK2/cyclin A/ATP, pT14pT160-CDK2/cyclin A/ATP/HHASPRK, pY15pT160-CDK2/cyclin A/ATP, and pY15pT160-CDK2/cyclin A/ATP/HHASPRK), and the CDK2–peptide substrate complex after the catalytic reaction has taken place (pT160-CDK2/cyclin A/ADP/HHApSPRK) (Table 1) were carried out using the SANDER module of the AMBER software package [22] with the *parm99* forcefield [23]. The starting geometries for simulations were prepared from available X-ray structures (PDB code: 1JST, 1QMZ, and 1GY3), and the Thr14 and Tyr15 residues were phosphorylated in silico using InsightII [24]. ATP is bound as a complex with Mg^{2+} and Mn^{2+} in the 1QMZ and 1JST crystal structures. Mn^{2+} was replaced by Mg^{2+} in the 1JST crystal structure. The MD simulation protocol was as follows: first, the protonation states of all histidines were checked by WHATIF [25] to create an optimal H-bond network. All hydrogens were added using the Xleap program from the AMBER software package [26]. The structures were neutralised by adding Cl^- counterions (see Table 1). Each system was inserted into a rectangular water box with a layer of water molecules equal to 10 Å. Then, each system was energy minimised prior to the production part of the MD run, which was carried out as follows: the protein was frozen and the solvent molecules with counterions were allowed to move during a 1,000-step minimisation and a 2 ps long MD run under NpT conditions. Then, the side chains were relaxed by several consequent minimisations with decreasing force constants applied to the backbone atoms. After relaxation, the system was heated to 250 K for 10 ps and then to 298.15 K for 40 ps. The production phases were run for 60 ns in total for all studied systems. The size of the studied systems, in which CDK is in complex with cyclin A, was ~60,000 atoms and the simulation period was chosen as a compromise between the quality of configuration space sampling and the calculation length. The 2 fs time integration step and particle-mesh Ewald (PME) methods for treating electrostatic interactions were used. All simulations were run under periodic boundary conditions in the NpT ensemble at 298.16 K and at a constant pressure of 1 atm. The SHAKE algorithm with a tolerance of 10^{-5} Å was applied to fix all bonds containing hydrogen atoms. A 10.0 Å cutoff was applied to treat non-bonding interactions. Coordinates were stored every 2 ps. All analyses of MD simulations were carried out by the CARNAL, ANAL, and PTRAJ modules of AMBER-8.0 [22], and by GROMACS [27]. Parameterisation of the phosphorylated threonine, serine, and tyrosine residues was prepared according to the standard scheme of Cornell et al. [28]. The MD simulation protocol and parameterisation of the phosphorylated tyrosine residue are described in detail elsewhere [29, 30].

Table 1 Summary of molecular dynamics (MD) simulations performed on cyclin-dependent kinase-2 (CDK2) complexes

System		PDB structure used	t (ns)	Number of Cl^- counterions
pT160-CDK2/cA/ATP[a]	Fully active	1JST	2.5	15
pT160-CDK2/cA/ATP/HHASPRK	Fully active CDK2 in complex with HHASPRK	1QMZ	15	17
pT14- and pY15pT160-CDK2/cA/ATP	Fully active CDK2 phosphorylated on inhibitory sites in the G-loop	1JST[b]	2×3	13
pT14- and pY15pT160-CDK2/cA/ATP/HHASPRK	Fully active CDK2 phosphorylated on inhibitory sites in the G-loop	1QMZ[b]	2×10	15
pT160-CDK2/cA/ADP/HHApSPRK	CDK2-HHASPRK complex after phospho-group transfer	1GY3	15	8

[a] Cyclin A is denoted as cA
[b] 1JST and 1QMZ crystal structures were modified by in silico phosphorylation at Thr14/Tyr15 in the G-loop

Results and discussion

Fully active CDK2

During the simulation of fully active CDK2, the conformation of the ATP phosphate moiety changes but the key features required for catalysis remain intact [29, 31]. The conformational change leads to a shift of α and β phosphate moieties while the γ phosphate, which is transferred to a substrate, remains in its position (Fig. 2). This orientation of the ATP phosphate moiety to the S_0 hydroxyl group is suitable for the catalytic reaction. The average distance S_0–O_γ…P_γ–ATP between the ATP terminal γ-phosphate group (P_γ) and the phosphorylation serine hydroxyl group (terminal O_γ atom) of the peptide substrate is 3.7±0.7 Å, which agrees well with the same distance measured in the X-ray crystal structure (PDB code 1QMZ [19]), i.e. 3.7 Å. The Mg^{2+} ion is hexacoordinated by oxygen atoms from the ATP phosphate moiety ($O_{\alpha 2}$, $O_{\beta 1}$, and $O_{\gamma 2}$ atoms), Asn132 $O_{\delta 1}$ and Asp145 $O_{\delta 2}$ oxygen atoms, and one water molecule oxygen during the whole production part of the MD simulation. Reconformation of ATP during the MD simulation leads to a change in the Mg^{2+} coordination sphere, when the initial coordination of the Mg^{2+} ion by the ATP $O_{\beta 3}$ atom is replaced by the ATP $O_{\beta 1}$ atom.

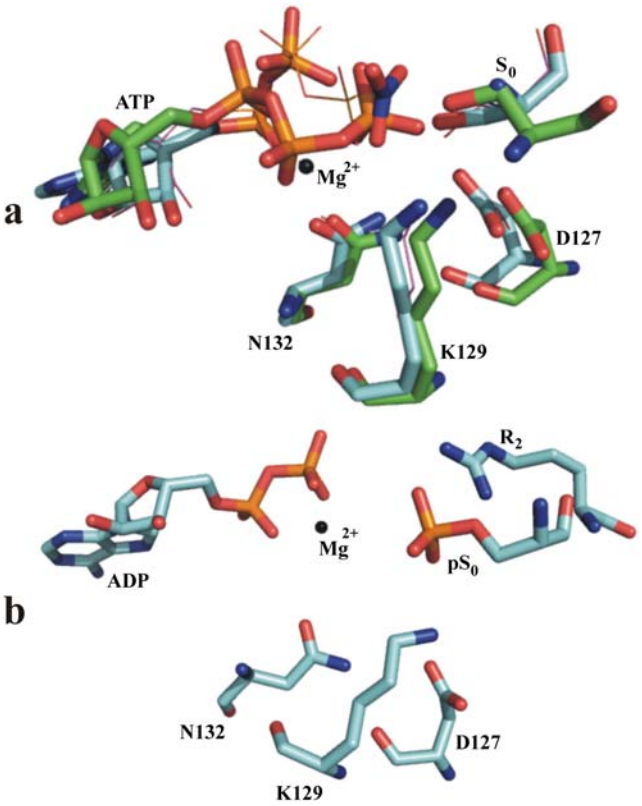

Fig. 2 The catalytic site of CDK2 in complex with substrate and in the transition state (TS) mimetic form. **a** ATP, S_0 serine from the peptide substrate, Asp127, Asn132, and Lys129 are shown in *licorice representation* coloured by element (C atoms in *green*) from a snapshot of the end of the MD simulation of fully active CDK2. *Wires* represent the same region of the crystal structure of the fully active CDK2 in complex with the substrate peptide (PDB ID 1QMZ) [19]. The crystal structure of the TS mimetic complex of pT160-CDK2/cyclin A with Mg^{2+}-ADP, nitrate and peptide substrate (PDB ID 1GY3) [34] is shown in *licorice representation* coloured by element (C atoms in *blue*). **b** Conformation and orientation of the ADP-Mg^{2+}, Asp127, Lys129, Asn132, peptide substrate pS_0, and arginine R_{+2} from the end of the MD simulation of the CDK2-peptide substrate after phospho-group transfer

Recently, De Vivo et al. [32] published a computational study dealing with the phosphoryl transfer reaction catalysed by the CDK2 enzyme, and identified deprotonation of the hydroxyl group of the S_0 peptide substrate side chain as a requisite chemical step during this catalysis. All protein kinases have a conserved catalytic aspartate residue in the C-terminal domain (Asp127 in CDK2), which is considered as the key residue playing the role of general base in the catalysis. A computational study by Cheng et al. [33] proved that the conserved aspartate serves as the general base in the catalytic reaction of cAMP-dependent protein kinase (PKA). The calculations of De Vivo et al. [32] indicated that Asp127 is deprotonated in the active form; however, these results do not directly support a role for Asp127 as the general base during the reaction mechanism, because it is too far from the catalytic site region to be involved as the general base in the reaction. These authors point out that Asp127 does not assist substrate serine hydroxyl group deprotonation, and they suggest an alternative associate mechanism, where protons are transferred from the substrate hydroxyl group to the ATP γ-phosphate in a concerted fashion with the phosphoryl transfer. In our MD simulations of active CDK2 in complex with the peptide substrate HHASPRK, the distance between Asp127-$O_{\delta 2}$ and $O_\gamma - S_0$ measured from the end of the MD simulation is equal to 5.0±0.5 Å, i.e., beyond the threshold for an H-bond (Fig. 2a). During the MD simulation of the CDK2–peptide substrate, Asp127 $O_{\delta 1/2}$ is H-bonded to the conserved lysine, Lys129 N_ξ (Table 2). The measured distance between Lys129-N_ξ…$O_{\delta 2}$-Asp127 during the production part of the MD simulation is equal to 2.8±0.1 Å. Lys129 N_ξ remains H-bonded to Asp127 $O_{\delta 2}$ in the CDK2–peptide substrate complex after the phosphoryl transfer reaction with the same average distance value. In this system (after reaction) the Lys129 side-chain forms additional H-bonds to the threonine Thr165 hydroxyl and to the pS_0 phosphate group. The mean distances Lys129-N_ξ…$O_{\gamma 1}$-Thr165 and Lys129-N_ξ…O_γ-pS_0 are equal to 2.9±0.1 Å and 2.8±0.1 Å, respectively. In the X-ray structure of the CDK2–substrate complex (PDB code: 1QMZ [19]) and crystal structure of the transition state (TS) analogue of this

Table 2 H-bond network in the CDK2 active site. Occupancy of observed hydrogen bonds, when H-bond distance is below the value of 3.50 Å, is shown in percent and average distances of H-bond contacts are shown in Ångstroms

	X-ray structures		MD structures			
			Fully active CDK2 in complex with HHASPRK	CDK2 phosphorylated at Thr14	CDK2 phosphorylated at Tyr15	CDK2 after phospho-group transfer
H-bond network in the CDK2 active site	1QMZ	1GY3 (TS)	pT160-CDK2/cA/ATP/ HHAS**$_0$**PRK[a]	**pT14**pT160-CDK2/ cA/ATP/ HHA**S$_0$**PRK	**pY15**pT160-CDK2/ cA/ATP/ HHA**S$_0$**PRK	pT160-CDK2/cA/ ADP/ HHA**pS$_0$**PRK
			Occupancy [%] Average distance [Å]			
K129 N_ξ…$O_{\delta 1/2}$ D127			84.9 2.8±0.1	77.3 2.8±0.1	79.8 2.9±0.2	97.8 2.8±0.1
K129 N_ξ…$O_{\delta 1}$ N132			0.3 3.0±0.2	89.3 2.8±0.1	76.3 2.8±0.1	23.5 2.9±0.1
N132 $N_{\delta 2}$…O D127			50.7 2.9±0.1	26.8 3.0±0.2	19.8 2.9±0.2	73.2 2.9±0.1
N132 $N_{\delta 2}$…$O_{\delta 1/2}$ D127		x[b]	4.5 3.0±0.2	97.5 2.9±0.1	83.5 2.9±0.1	8.2 2.9±0.2
N132 N…O K129			92.7 3.0±0.1	99.4 2.9±0.1	95.6 2.9±0.1	94.3 2.9±0.1
T165 $O_{\gamma 1}$…$O_{\delta 1/2}$ D127		x	97.5 2.7±0.1	19.5 2.7±0.2	27.0 2.7±0.1	47.9 2.8±0.2
T165 $O_{\gamma 1}$…N_ξ K129		x	19.3 2.9±0.1	1.5 3.0±0.2	7.8 3.0±0.2	61.8 2.9±0.1
T165 $O_{\delta 1}$ D127			60.2 3.0±0.2	15.3 3.1±0.2	19.5 3.0±0.2	81.7 3.0±0.2
S_0 O_γ… $O_{\delta 1/2}$ D127	x	x (A sub.)	0	0	42.0 2.6±0.1	——[c]
S_0 O_γ… N_ξ K129	x	x	2.3 3.0±0.1	1.4 3.0±0.2	7.0 3.0±0.2	——
K129 N_ξ…pS_0 O_γ			——	——	——	97.9 2.8±0.1

[a] Bold face indicates residues that were phosphorylated or dephosphorylated in studied systems
[b] H-bond that occurs in the X-ray structure
[c] Corresponding H-bond does not occur

complex (PDB code: 1GY3 [34]), the S_0 hydroxyl is positioned, by the conserved catalytic aspartate Asp127 and the lysine residue Lys129, via two H-bonds to Asp127 $O_{\delta 2}$ and Lys129 N_ξ. The distance between the Asp127 O_δ atom and the S_0 hydroxyl is equal to 2.7 Å in both subunits of the 1QMZ crystal structure, and 2.7 Å and 3.5 Å in the A and C subunits of the 1GY3 crystal structure, respectively. In the 1QMZ crystal structure, the Asp127 side-chain is in a suitable orientation to assist the catalytic reaction (likely as the general base), while Lys129 may assist in stabilising the negative charge of the transition state, as proposed for phosphorylase kinase (PhK) [35]. Combining all available data does not lead to a clear consensus about the role of the conserved aspartate, and more attention should be paid to this issue.

The lysine at the P_{+3} position of the peptide substrate HHASPRK is H-bonded to the pThr160 phosphate group during the whole simulation; the Arg (R_{+2}) side chain at the P_{+2} position moves toward the ATP phosphate moiety at ~2.8 ns, and its conformation then remains stable during the rest of the MD simulation. The preference of CDK2 for a basic residue $(R/K)_{+2}$ observed from kinetic experiments and crystallographic analysis cannot be deduced from the crystal structure, because R_{+2} makes no contact with the protein, having its side chain pointing towards the bulk solvent. In contrast, the R_{+2} side chain position observed in the MD simulation offers a possible explanation for this preference. The alternative R_{+2} conformation enables a direct interaction of R_{+2} with the ATP phosphate moiety and, consequently, it can also contribute to appropriate ATP alignment prior to the catalytic reaction. Another possible explanation is that the R_{+2} side chain could interact with the product pS_0 phosphate group after the phospho-group transfer, and could assist in product dissociation, preventing

pS_0 phosphate group interactions with CDK2 active site residues (see Fig. 2b).

The N-terminal substrate peptide moiety (HH residues at positions P_{-2} and P_{-3}) is flexible during the MD simulation; nevertheless, the H_{-2} makes an H-bond to the Asp206 side chain of the conserved CDK G**D**SEID motif. The glycine-rich loop (G-loop), whose residues are crucial for appropriate ATP alignment for phosphorylation [36], moves periodically during the MD simulation, causing gentle opening and closing of the substrate binding box. On the other hand, this movement does not affect the ATP conformation and orientation to the S_0 residue from the peptide substrate.

Inhibited CDK2

MD simulations of CDK2 inhibited by phosphorylation at Thr14 or Tyr15 in the G-loop provided the first clear insight into the structural aspects of CDK2 deactivation by phosphorylation [29, 31]. The simulations show that, in both cases, the inhibitory phosphorylation causes misalignment of the ATP phosphate moiety, changes in the Mg^{2+} ion coordination sphere, resulting in loss of Mg^{2+} ion coordination by Asn132 (a residue conserved in all protein kinases), and G-loop shift (~5 Å) away from the ATP binding site, which leads to opening of the substrate binding box. ATP misalignment, which results in reconformation of the terminal phospho-group is demonstrated by an increase in the S_0–O_γ…P_γ–ATP distance, whose average value is equal to 8.8±2.2 Å and 6.6±1.5 Å for CDK2 inhibited by phoshorylation at Tyr15 and Thr14, respectively. The lengths of S_0–O_γ…P_γ–ATP distances below 3.9 Å were calculated. The distance remains lower than the threshold for 87.7%, 9.6%, and 5.8% of the simulation time for the fully active CDK2 and CDK2 inhibited by phosphorylation at Tyr15 and Thr14 residues, respectively [31]. Changes in the CDK2 active site after CDK2 inhibition by phosphorylation in the G-loop, such as, e.g., reconformation of ATP and Asn132, cause changes in the H-bond network within the CDK2 active site (see Table 2). The Asn132 side chain creates a new H-bond to the conserved Lys129 residue and to the catalytic Asp127 side chain.

We have described the essential motions of several CDK2 forms related to its regulation [13]; the significant essential motions of CDK2 inhibited by phosphorylation at the inhibitory sites are located in the G-loop and accompany a movement of the G-loop away from the ATP binding site, which leads to opening of the active site and broadening of the substrate-binding site (Fig. 3).

Phosphorylation of residue Tyr15 causes the R_{+2} positively charged side chain to interact preferably with this group, and the interaction with ATP phosphates is lost (Fig. 3). On the other hand, the inhibitory phosphorylation

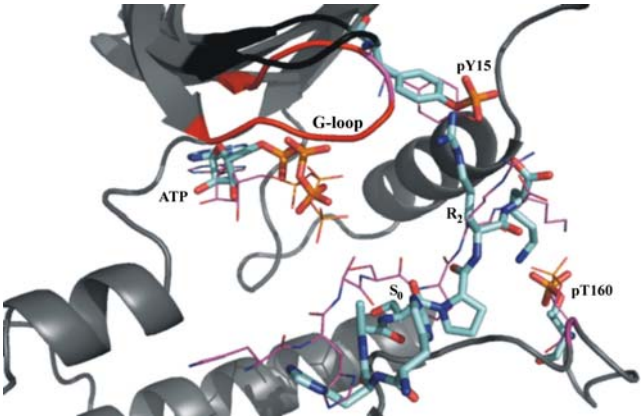

Fig. 3 G-loop shift and opening of the substrate binding box following inhibitory phosphorylation of residue Tyr15 in the G-loop. The CDK2 structure is drawn in *ribbon representation* and is coloured *grey*. The G-loop conformation is *black* in the inhibited pY15-CDK2 and *red* in the fully active CDK2 (MD equilibrated structure). pTyr15, pThr160, ATP, and peptide substrate (HHASPRK) are shown in *licorice representation* for the inhibited CDK2, and in *wire representation* for the fully active CDK2 (MD equilibrated structure)

at Thr14 or Tyr15 does not affect the interaction of K_{+3} with the pThr160 side chain at the available time scale. The phosphorylated Tyr15 residue may also weaken substrate binding or its correct alignment for ATP terminal phospho-group transfer to the CDK2 substrate.

All the effects mentioned above clearly explain the loss of kinase activity following inhibitory phosphorylation of the CDK2 G-loop, because correct coordination of the Mg^{2+} ion and appropriate orientation and conformation of the ATP phosphate moiety are crucial for phospho-group transfer to the serine (S_0) hydroxyl from the peptide substrate. Recently, Welburn et al. [37] presented the X-ray crystallographic analysis of CDK2/cyclin A phosphorylated on Tyr15 and Thr160 and thereby confirmed the main results of our MD studies [29, 31]. Phosphorylation also leads to a dramatic shift in the position of the γ-phosphate, which loses many important contacts for effective substrate phosphorylation. The presence of the phosphate group on the Tyr15 hydroxyl results in a slight opening of the active site cleft. However, crystallographic analysis shows that Tyr15 phosphorylation does not perturb the activation loop or the conformation of residues Lys33, Glu51, Asp127, Lys129, Asn132, and Asp145 that are involved in the phospho-transfer reaction [37]. On the other hand, the pY15pT160-CDK2 crystal structure (PDB ID 2CJM) reveals that the inhibitory phosphorylation at residue Tyr15 affects the Mg^{2+} ion coordination sphere, resulting in the loss of Mg^{2+} ion coordination by Asn132 and Asp145 residues. In the 2CJM crystal structure, the distance between Mg^{2+}…$O_{\delta 1}$–Asn132 is equal to 6.1 Å and distance between Mg^{2+}…$O_{\delta 2}$–Asp145 is equal to 5.8 Å.

Conclusions

A number of nanosecond-scale MD trajectories of differently active complexes of human CDK2 (fully active, and CDK2 inhibited by phosphorylation on inhibitory sites in the G-loop) and CDK2 in complex with peptide substrate HHASPRK (CDK2-HHASPRK complex before and after the phosphate transfer reaction) were produced and compared to aid the structural understanding of the role of Thr160 and Thr14/Tyr15 (de)phosphorylation in regulating CDK activity and to understand the role of catalytic (conserved) amino acids in the process of the catalytic reaction. The mechanism of CDK2 inhibition by phosphorylation on inhibitory sites in the G-loop was studied in detail; MD simulations provided valuable insight into the structural aspects of CDK2 deactivation. The catalytic function of CDKs is phosphorylation of a substrate protein via transfer of the γ-phosphoryl group of ATP to a threonine or serine (P_0) on the target protein substrate. Therefore, the correct coordination of the Mg^{2+} ion and appropriate conformation and orientation of the ATP phosphate group to the CDK2 substrate are important for ATP terminal phospho-group transfer. The position of the ATP γ-phosphate and catalytic residues relative to the serine at the P_0 phosphorylation site of the peptide substrate in the active CDK2 is described and compared with inhibited forms of CDK2. The inhibitory phosphorylation causes ATP reconformation and misalignment for phosphorylation, changes in the Mg^{2+} ion coordination sphere, and changes in the H-bond network formed by the catalytic residues within the CDK2 active site as well as a G-loop shift away from the ATP binding site, which leads to opening of the CDK2 substrate binding box [29, 31]. Such changes might decrease the affinity of CDK2 to its substrate or lead to the incorrect ATP orientation with respect to the S_0 hydroxyl. The phosphorylated Tyr15 residue likely weakens substrate binding or its correct alignment for ATP terminal phospho-group transfer to the CDK2 substrate. All these effects explain the 200-fold decrease in kinase activity after phosphorylation at Tyr15 in the G-loop [37].

Interactions of specific residues required for substrate (HHASPRK) binding to CDK2 were also studied with MD simulations and compared with the CDK2-HHApSPRK complex after phospho-group transfer. The MD structures confirmed why a basic residue is preferred at the P_{+3} substrate position. This residue is H-bonded to the pThr160 phosphate during the whole production part of each studied CDK2 complex. These results broaden hypotheses drawn from our previous MD studies as to why a basic residue (Arg/Lys) is preferred at the P_{+2} peptide substrate position. The R_{+2} either interacts with the ATP phosphate moiety and, therefore, plays a role in appropriate ATP alignment before the catalytic reaction [31] or, after the catalytic reaction, the R_{+2} side chain interacts with the pS_0 phosphate group and weakens the interaction of this moiety with CDK. Consequently, it can facilitate product release from the substrate-binding box of CDK.

Acknowledgements We thank the Meta Center (http://meta.cesnet.cz) for computer time. The Czech Ministry of Education is acknowledged for financial support; grants: MSM6198959216, MSM0021622413 and LC06030.

References

1. Morgan DO (1997) Annu Rev Cell Dev Biol 13:261–291
2. Morgan DO (1995) Nature 374:131–134
3. Gould KL, Nurse P (1989) Nature 342(6245):39–45
4. Morla AO, Draetta G, Beach D, Wang JYJ (1989) Cell 58(1):193–203
5. Takizawa CG, Morgan DO (2000) Curr Opin Cell Biol 12(6):658–665
6. Gu Y, Rosenblatt J, Morgan DO (1992) EMBO J 11:3995–4005
7. Sebastian B, Kakizuka A, Hunter T (1993) Proc Natl Acad Sci USA 90:3521–3524
8. Watanabe N, Broome M, Hunter T (1995) EMBO J 14(9):1878–1891
9. Manning G, Whyte DB, Martinez R, Hunter T, Sudarsanam S (2002) Science 298:1912–1934
10. Knockaert M, Greengard P, Meijer L (2002) Trends Pharmacol Sci 23(9):417–425
11. Meijer L, Raymond E (2003) Acc Chem Res 36(6):417–425
12. Kannan N, Neuwald AF (2004) Prot Sci 13(8):2059–2077
13. Bártová I, Koča J, Otyepka M (2008) Prot Sci 17:22–33
14. De Bondt HL, Rosenblatt J, Jancarik J, Jones HD, Morgan DO, Kim SH (1993) Nature 363:595–602
15. Jeffrey PD, Russo AA, Polyak K, Gibbs E, Hurwitz J, Massague J, Pavletich NP (1995) Nature 376:313–320
16. Brown NR, Noble MEM, Lawrie AM, Morris MC, Tunnah P, Divita G, Johnson LN, Endicott JA (1999) J Biol Chem 274:8746–8756
17. Morris MC, Gondeau C, Tainer JA, Divita G (2002) J Biol Chem 277(28):23847–23853
18. Russo AA, Jeffrey PD, Pavletich NP (1996) Nat Struct Biol 3:696–700
19. Brown NR, Noble MEM, Endicott JA, Johnson LN (1999) Nat Cell Biol 1:438–443
20. Songyang Z, Blechner S, Hoagland N, Hoekstra MF, Piwnica-Worms H, Cantley LC (1994) Curr Biol 4(11):973–982
21. Holmes JK, Solomon MK (1996) J Biol Chem 271(41):25240–25246
22. Case DA, Darden TA, Cheatham III TE, Simmerling CL, Wang J, Duke RE, Luo R, Merz KM, Wang B, AMBER 8. 2004: University of California, San Francisco
23. Wang JM, Cieplak P, Kollman PA (2000) J Comput Chem 21 (12):1049–1074
24. Insight II. In Homology Model, Accelrys Inc.: San Diego
25. Vriend G, WHAT IF. 1997, EMBL: Heidelberg
26. Case DA, Pearlman DA, Caldwell JW, Cheatham III TE, Ross WS, Simmerling CL, Darden TA, Merz KM, Stanton RV, AMBER 6 1999: University of California, San Francisco
27. Spoel DVD, Buuren ARV, Apol E, Meulenhoff PJ, Tieleman PD, Sijbers ALTM, Hess B, Feenstra KA, Lindhal E, GROMACS. 1991–2002, University of Groningen: Groningen

28. Cornell WD, Cieplak P, Bayly CI, Gould IR, Merz JKM, Ferguson DM, Spellmeyer DC, Fox T, Caldwell JW (1995) J Am Chem Soc 117:5179–5197
29. Bártová I, Otyepka M, Kříž Z, Koča J (2004) Prot Sci 13:1449–1457
30. Otyepka M, Bartova I, Kriz Z, Koca J (2006) J Biol Chem 281 (11):7271–7281
31. Bártová I, Otyepka M, Kříž Z, Koča J (2005) Prot Sci 14:445–451
32. De Vivo M, Cavalli A, Carloni P, Recanatini M (2007) Chem Eur J 13:8437–8444
33. Cheng Y, Zhang Y, McCammon JA (2005) J Am Chem Soc 127 (5):1553–1562
34. Cook A, Lowe ED, Chrysina ED, Skamnaki VT, Oikonomakos NG, Johnson LN (2002) Biochemistry 41:7301–7311
35. Skamnaki VT, Owen DJ, Noble MEM, Lowe ED, Lowe G, Oikonomakos NG, Johnson LN (1999) Biochemistry 38 (44):14718–14730
36. Hanks S, Quinn AM (1991) Methods Enzymol 200:38–62
37. Welburn JPI, Tucker JA, Johnson T, Lindert L, Morgan M, Willis A, Noble MEM, Endicott JA (2007) J Biol Chem 282(5):3173–3181